Molecular Dynamics Study on Sensitivity Criterion, Thermal Expansion and Mechanical Properties of Multi-component High Energy Systems

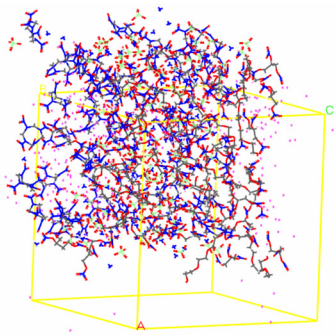

The models of a five-component system ((PEG/NG/BTTN)/AP/HMX) with four sets of proportion and a six-component system ((PEG/NG/BTTN)/AP/HMX/Al) were designed and established. The safety performance, thermal expansion and mechanical properties of these complicated systems were explored by molecular dynamics simulation.

ZHU Wei, LIU Dong-mei, XIAO Ji-jun, ZHAO Xiao-bin, ZHENG Jian, ZHAO Feng, XIAO He-ming

Chinese Journal of Energetic Materials, **2014**, **22**(**5**): **582–587**

Molecular Dynamics Simulation on the Compatibilities of HTPE/Plasticizer Mixtures

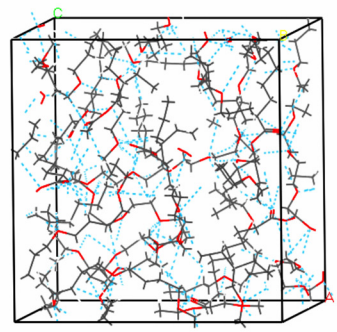

The compatibilities of HTPE with DBP, DOS and DEP were studied by molecular dynamics simulation method. By analysing the binding energy, radial distribution function and glass transition temperature, the compatibility of the polymer binder with the plasticizer could be predicted.

CAI Jia-lin, ZHENG Shen-sheng, ZHENG Bao-hui, LUO Guan

Chinese Journal of Energetic Materials, **2014**, **22**(**5**): **588–593**

Effects of Multi-point Initiation Charge Configuration Parameters on EFP with Fins Formation

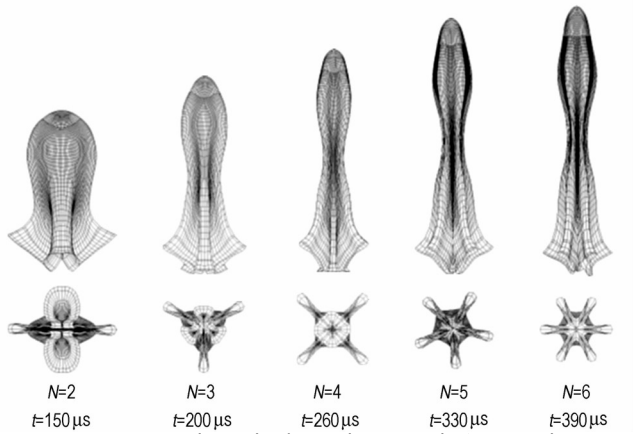

Multi-point initiation explosively formed projectile (EFP) charges with different N (the number of initiation points), D_I (the diameter of annular initiation), L_C/D_C (the length/diameter of charge) were studied by LS-DYNA program. Shapes of EFP with fins formed by different numbers of initiation points ($N=2-6$) were approached by numerical simulation. The number of fins was equal to the number of initiation points.

LIU Jian-qing, GU Wen-bin, XU Hao-ming, LU Ming, WU Shuang-zhang

Chinese Journal of Energetic Materials, **2014**, **22**(**5**): **594–599**

Test and Three-dimensional Numerical Simulation of Penetrating Steel Ingot by Linear Shaped Charge with Oval Cover

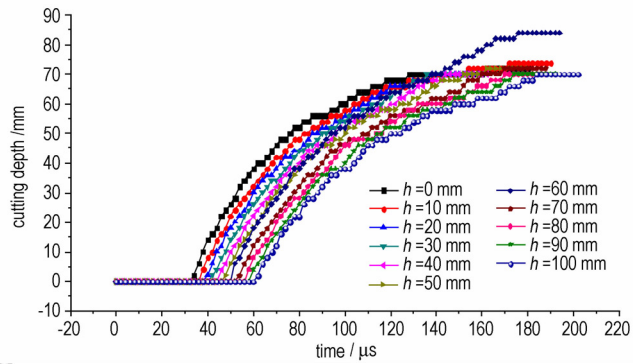

The characteristics and laws of penetrating steel ingot of linear shaped charge(LSC) with oval cover were studyed by using the method of test and three-dimensional numerical simulation. The results of numerical simulation were consistent with the test results. The characteristics and laws of penetrating steel ingot obtained by using the methods of three-dimensional numerical simulation can better reflect the actual cutting process.

WU Shuang-zhang, GU Wen-bin, LIU Jian-qing, LI Xu-feng
Chinese Journal of Energetic Materials,2014,22(5): 600–606

Jet Impact Initiation of the Charge Covered with Spaced Target

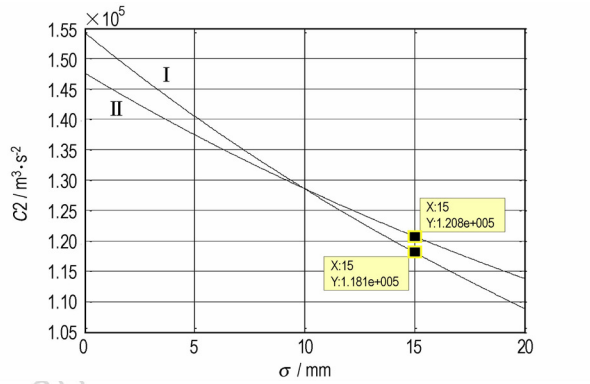

The initiation model of jet impact charge covered with spaced target was established. The model was used to calculate the detonating abilities of shock wave and remainder jet by two examples Ⅰ and Ⅱ.

ZHANG Jun-kun, GAO Xin-bao, XIONG Ran, XING Na
Chinese Journal of Energetic Materials,2014,22(5): 607–611

Numerical Simulation on Influence of Reinforced Concrete Thickness on PELE Penetration

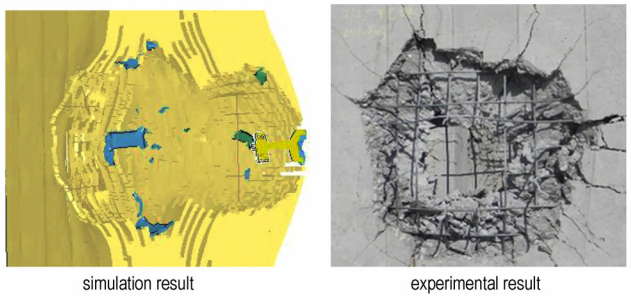

The simulated and experimental results while penetrator with enhanced lateral effect(PELE) penetrated the 50 cm thickness reinforced concrete targets with the velocity of 800 m·s^{-1}.

YE Xiao-jun, DU Zhong-hua, YAO Fang-tang
Chinese Journal of Energetic Materials,2014,22(5): 612–616

Numerical Simulation of Heat Transfer Problems in Structure with Explosive under Fire

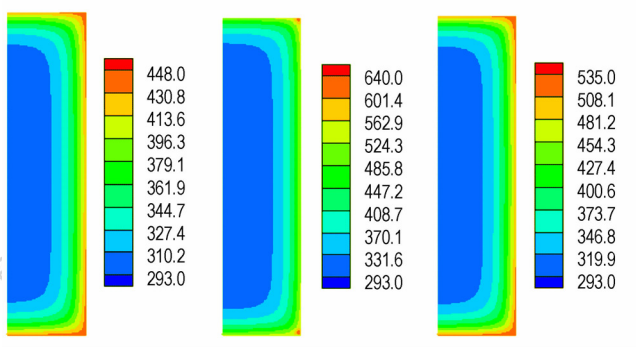

The numerical models of poor fire's temperature rise heat transfer, carbon/bakelite ablatant's high temperature endothermic decomposition, inner air layer's complex heat transfer and explosive's exothermic decomposition were established. The thermal response and thermal ignition delay time for the structure with explosive under the conditions of different temperature (constant value 1073 K, 1273K, measured temperature rise curve proposed in this work), different fire's emissivity (0.1–0.9) and different surface emissivity for the shell with different air gap (0.1–0.9) were calculated and obtained using the established numerical models.

WU Song, LI Ming-hai, ZHANG Zhong-li

Chinese Journal of Energetic Materials,**2014**,**22**(**5**): **617–623**

Multi-objective Optimization for Waterjet Cleaning Process of Solid Rocket Motor

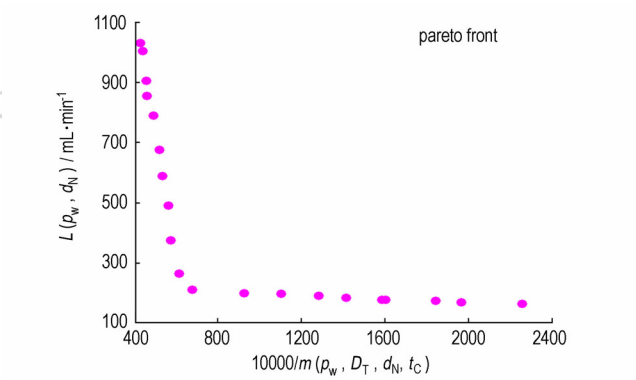

A multi-objective optimization method for waterjet cleaning process of solid rocket motor was established with propellant massloss rate and wastewater generation rate as the optimization objectives, and waterjet pressure, target distance, nozzle diameter and single cleaning time as the variables.

ZHU Zuo-ming, GAO Xin, WANG Xuan-jun, HAN Qi-long

Chinese Journal of Energetic Materials,**2014**,**22**(**5**): **624–629**

Degradation Kinetic Study of UDMH by Flora FYD

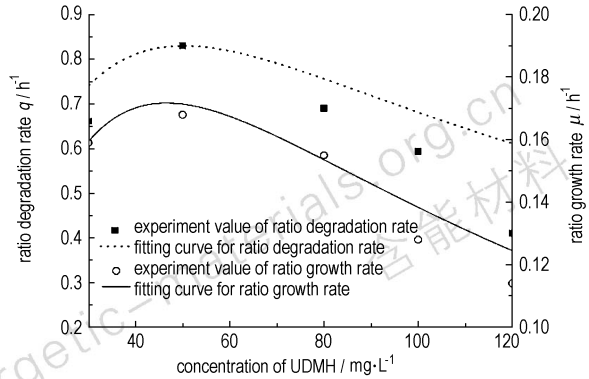

FAN Chun-hua, WANG Li, XIA Ben-li, XIE Shan-shan, LI Jian-wei

Chinese Journal of Energetic Materials, 2014, 22(5): 630–634

The growth kinetic process of efficient bacteria flora (FYD) for degrading unsymmetrical dimethyl hydrazine (UDMH) was simulated by Haldane kinetic model of growth inhibition. The degradation kinetic process of UDMH was simulated by Andrews noncompetitive kinetic model of substrate inhibition.

Preparation, Thermal Decomposition Mechanism and Combustion Catalytic Activity of Zirconium 3,5-dinitrosalicylate (DNS-Zr)

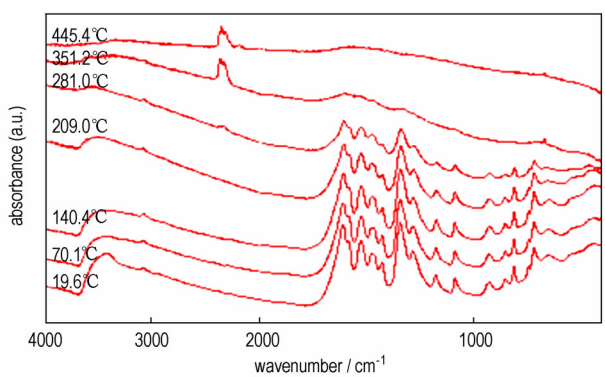

ZHAO Feng-qi, ZHANG Heng, AN Ting, ZHANG Xiao-hong, GAO Hong-xu, SONG Xiu-duo

Chinese Journal of Energetic Materials, 2014, 22(5): 635–640

Zirconium 3,5-dinitrosalicylate (DNS-Zr) was synthesized and characterized. The thermal behavior and decomposition mechanism of DNS-Zr were investigated byTG-DTG, DSC and condensed phase thermolysis/FTIR techniques. The effects of DNS-Zr on combustion properties of DB/CMDB propellants were studied.

Effect of Several Burning Rate Catalysts on the Thermal Decomposition Properties of P(BAMO/AMMO) Energetic Binder

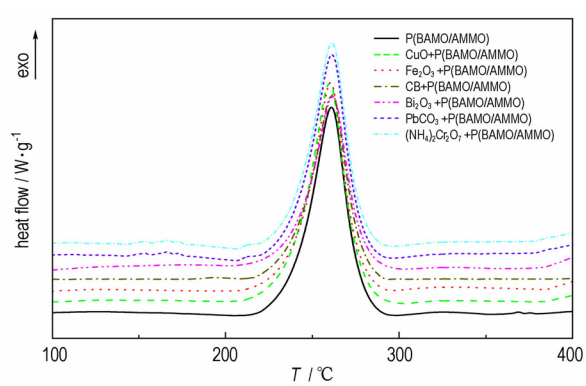

WANG Gang, GE Zhen, LUO Yun-jun

Chinese Journal of Energetic Materials, 2014, 22(5): 641–645

Effects of CuO, Fe_2O_3, CB, $PbCO_3$, Bi_2O_3 and $(NH_4)_2Cr_2O_7$ on the thermal decomposition properties of P(BAMO/AMMO) energetic binder were studied by TG and DSC.

Synthesis, Characterization and Crystal Structure of 2,2,4,4,6,6-Hexanitroadamantane

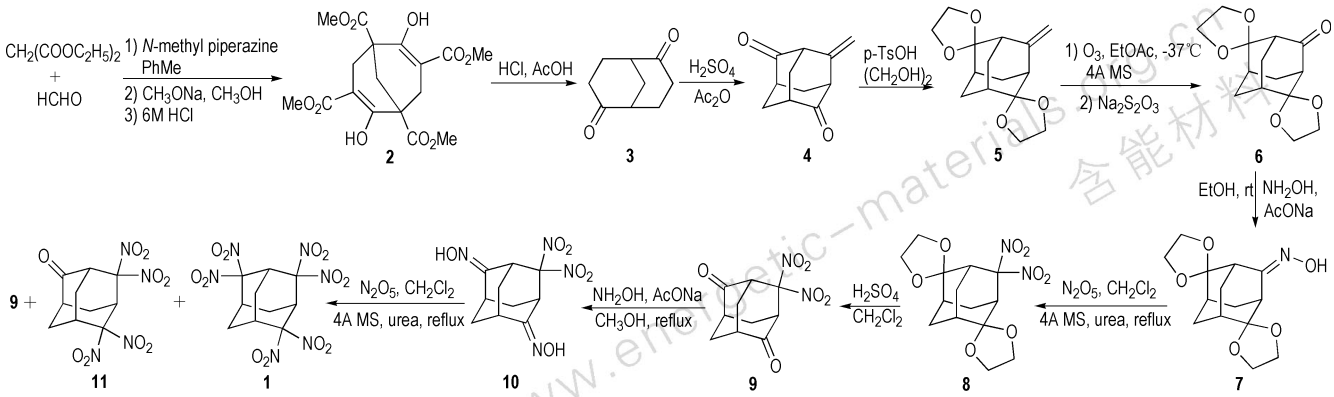

2,2,4,4,6,6-Hexanitroadamantane was synthesized with a total yield of 3% using diethyl malonate and paraformaldehyde as raw materials by a process including cyclization, decarboxylation, ozonation, oximation and oxidative nitration.

ZHANG Ping-ping, LING Yi-fei, SUN Lu, LUO Jun

Chinese Journal of Energetic Materials, 2014, 22(5): 646–653

Synthesis, Crystal Structure and Thermal Property of 1-Amino-3, 5-dinitropyrazole

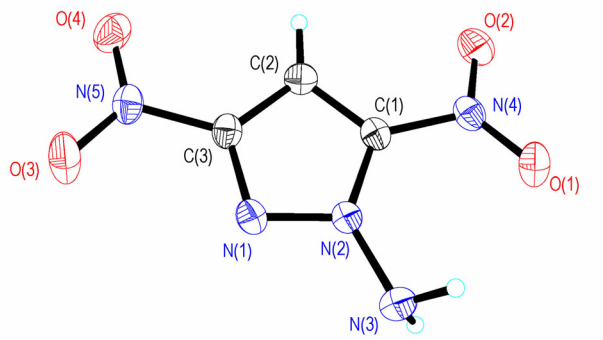

1-Amino-3, 5-dinitropyrazole (ADNP) was synthesized using 3, 5-dinitropyrazole as raw material and 2,4,6-trimethylbenzenesulfonic hydroxylamine (MSH) as aminating agent. Its structure was characterized by IR, NMR, MS and element analyses. The single crystal of ADNP was cultivated in ethanol and its single crystal structure was determined by a four-circle X-ray diffractometer. Its thermal property was studied by TG-DSC.

JIANG Tao, ZHANG Xiao-yu, JING Mei, SHU Yuan-jie, WANG Jun

Chinese Journal of Energetic Materials, 2014, 22(5): 654–657

Dynamic Mechanics Response and Mesoscopic Damage of a PBX Simulant

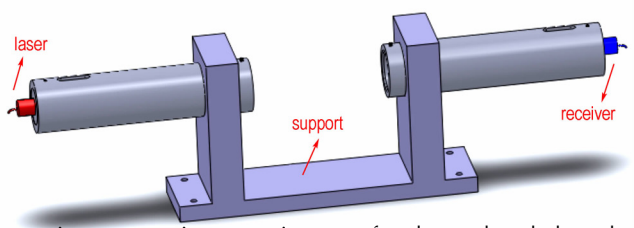

The dynamic compression experiments of polymer bonded explosive (PBX) simulants were performed under high strain rates (1763 ~ 2650 s^{-1}) loading by using a modified SHPB device. The axial strain of the specimens was monitored by the laser displacement meter. Mesoscopic structure morphology and damage model of the specimen were observed by electron microscope.

CAI Xuan-ming, ZHANG Wei, WEI Gang, REN Peng, HUANG Wei

Chinese Journal of Energetic Materials, 2014, 22(5): 658–663

Related Parameters of Interfacial Interaction between F2314/AS Composite Binder and TATB

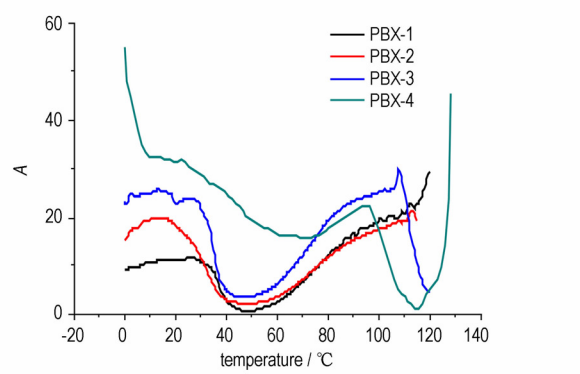

Based on different theoretical models, the interfacial interaction between fluoropolymer F2314/acrylonitrile-styrene copolymer (AS) composite and TATB was evaluated to explore the effects of component and proportion of binder on interfacial interaction of polymer bonded explosive (PBX).

LIN Cong-mei, LIU Jia-hui, LIU Shi-jun, HUANG Zhong, LI Yu-bin, ZHANG Juan, PAN Li-ping, ZHANG Jian-hu

Chinese Journal of Energetic Materials, 2014, 22(5): 664-668

Experimental Study of Thermal Physical Property of Aged AP/HTPB Composite Base Bleed Propellant

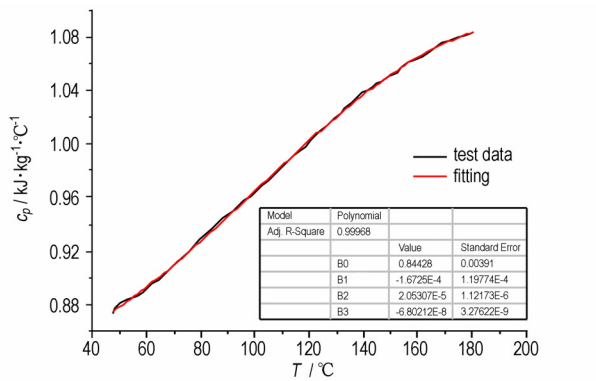

The specific heat capacity and conductivity coefficient for unaged and naturally aged (stored in a sealed plastic bag under room temperature) AP/HTPB base bleed propellant used in a 155 mm base bleed projectile were determined by differential scanning calorimeter (DSC) and conductometer.

ZHANG Ling-ke, ZHAP Wei, YU Yong-gang

Chinese Journal of Energetic Materials, 2014, 22(5): 669-673

Influence of Compressive Stress on Annular Gap Defect of Casting-PBX Charge

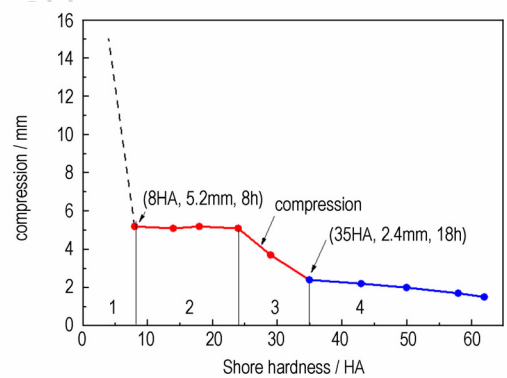

The influence of compressive stress and Shore hardness on the annular gap defect of a casting polymer bonded explosive (P-1 explosive) charge after curing was studied using a compression technology. The relationship between stress and strain was analyzed. The fitting equation of stress-strain for P-1 explosive in compression curing process was obtained. The CT detection of the explosive was carried out.

XI Peng, WANG Xiao-feng, ZHENG Ya-feng, NAN Hai, GUO Xin, YANG Jian-gang

Chinese Journal of Energetic Materials, 2014, 22(5): 674-677

Effect of Aluminum Film Content on Underwater Explosion Performance of RDX-based Aluminum Film Explosive

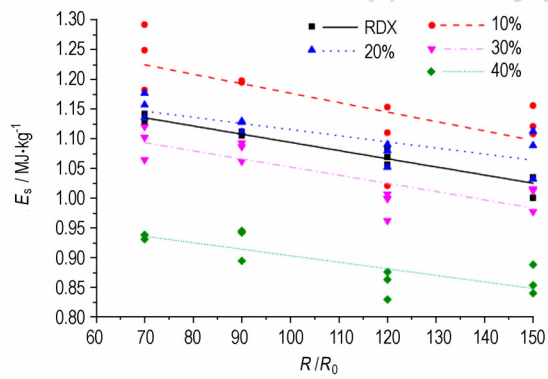

LIN Mou-jin, MA Hong-hao, SHEN Zhao-wu, YU Yong

Chinese Journal of Energetic Materials, **2014**, **22**(**5**): **678–683**

Aluminum film explosive was proposed by replacing aluminum powder in traditional aluminized explosives with aluminum film. The pressure-time curves at different position for composite explosives with aluminum film content of 10% – 40%, and RDX were obtained by underwater explosion contrast experiments. The peak pressure, impulse, specific shock wave energy and specific bubble energy were obtained.

Experimental Research on Energy Output of Thermobaric Explosive

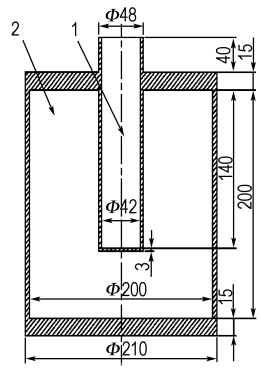

LU Yong, WANG Bo-liang, HE Zhong-qi, LI Xi, LIU Bo

Chinese Journal of Energetic Materials, **2014**, **22**(**5**): **684–687**

The double-layer test device filled with different gases was used to study the effects of the explosion energy outputs of thermobaric explosives under closed condition. The experiment was studied by an underwater explosion test method, the inner container was used to place the explosives, and the outer container was used to fill different gases under different pressures.

Structural Design and Numerical Simulation on the Piston Micro-actuator

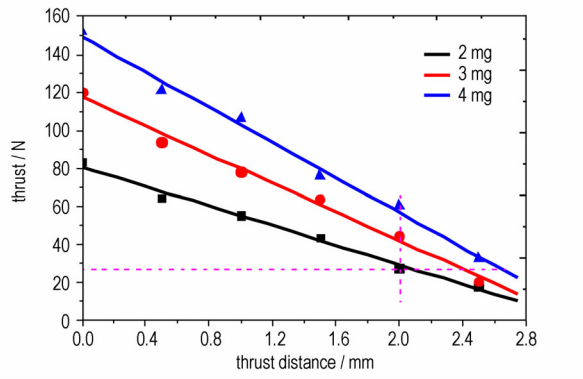

ANSYS/LS-DYNA finite element software was applied to analyze the structure design of the piston micro-actuator, and the structure and size parameters which affect its performance were determined. The anti-thrust force and setback force of different structural size parameters piston micro-actuators was obtained through the piston micro-actuator performance experimental test.

YAN Nan, WANG Gang, GENG Wan-jun, ZHANG Liang
Chinese Journal of Energetic Materials, 2014, 22(5): 688–692

Explosives with Structure of Honeycomb and its Application

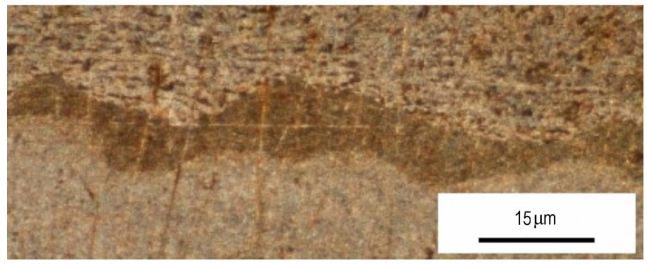

Explosives with structure of honeycomb was prepared to ensure the quality of charge, and applied to double side explosion cladding to clad two combination plates.

MIAO Guang-hong, MA Hong-hao, SHEN Zhao-wu, YU Yong
Chinese Journal of Energetic Materials, 2014, 22(5): 693–697

Thermal Behavior of Non-explosive and Irrestorable Fertilizer-grade Ammonium Nitrate

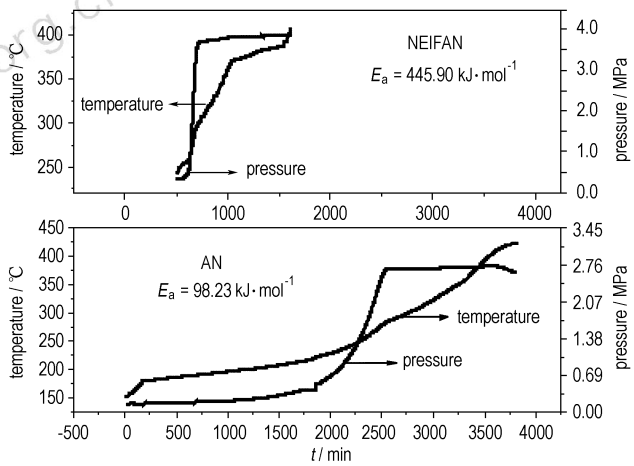

The crystal transformation changes, thermal decomposition characteristics and adiabatic decomposition processes of AN and NEIFAN were studied by TA-DTA-DTG, DSC and ARC.

SHEN Li-jin, MA Ai-e, WANG Xu-guang, WANG Ping
Chinese Journal of Energetic Materials, 2014, 22(5): 698–701

Treatment of Nitrobenzene-containing Wastewater Using Different Combined Processes with Ozone

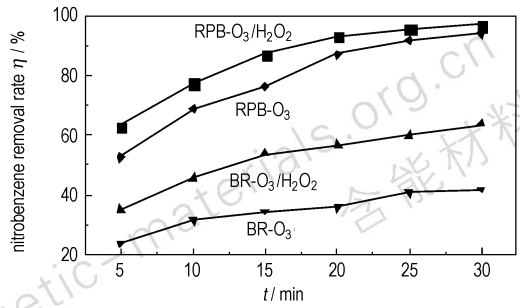

GUO Liang, JIAO Wei-zhou, LIU You-zhi, XU Cheng-cheng, LIU Wen-li, LI Jing

Chinese Journal of Energetic Materials, 2014, 22(5): 702-708

Four combined processes of RPB-O_3/H_2O_2, RPB-O_3, BR-O_3/H_2O_2 and BR-O_3 were experimentally conducted to treat nitrobenzene compounds in simulated wastewater.

Progress of *N*, *N*′-Bis(1(2)*H*-Tetrazol-5-yl)amine and its Derivatives

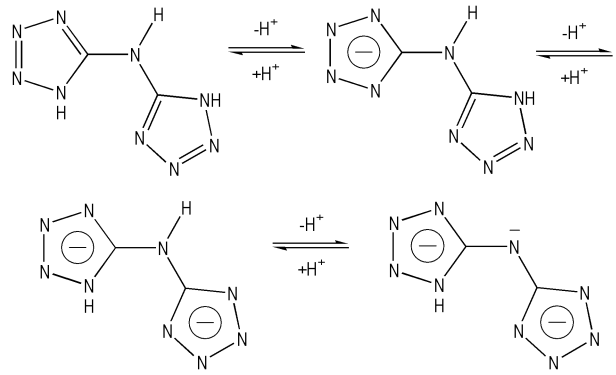

GAO Fu-lei, CHEN Bin, FAN Hong-jie, WANG Ying-lei, LIU Wei-xiao, LIU Ya-jing, JI Yue-ping

Chinese Journal of Energetic Materials, 2014, 22(5): 709-715

The progress of *N*, *N*-bis(1(2)*H*-tetrazol-5-yl)amine (H_2BTA) and its derivatives were briefly reviewed, especially the synthesis, performance and application investigation of H_2BTA based energetic materials.

Compatibility of Dihydroxylammonium 5,5′-Bistetrazole-1,1′-diolate with Components of CMDB Propellant

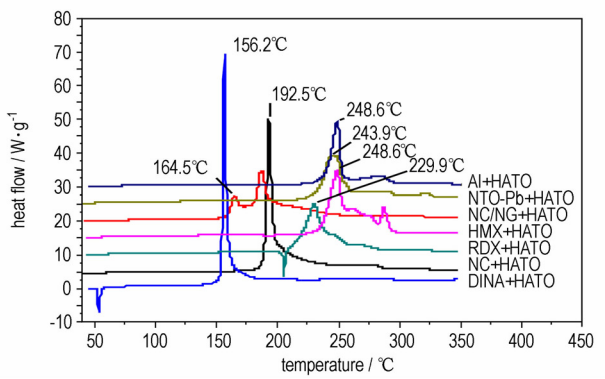

BI Fu-qiang, GE Zhong-xue, SUN Xu-dong, HAN Fang, FAN Xue-zhong, WANG Wei, JU Rong-hui

Chinese Journal of Energetic Materials, 2014, 22(5): 716-718

The compatibilities of dihydroxylammonium 5,5′-bistetrazole-1,1′-diolate (HATO) with components of CMDB propellant components, including NC, NC/NG, DINA, RDX, HMX, NTO-Pb and Al powder were studied by DSC and VST.

Convenient Synthesis of $B(N_3)_3$

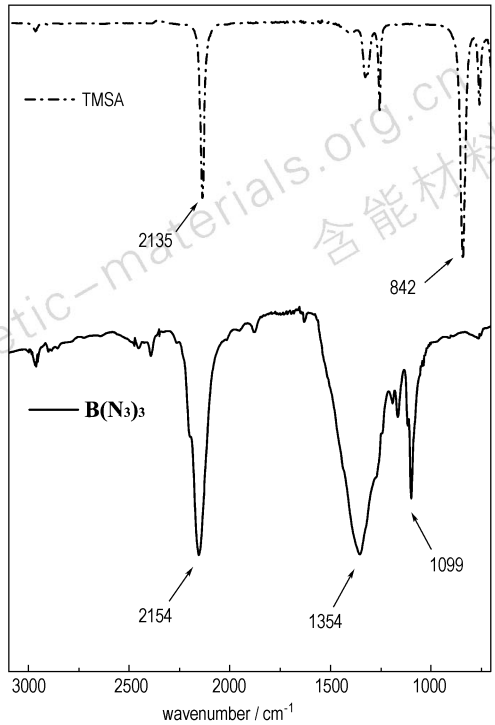

DING Ke-wei, LI Tao-qi, JI Xiao-tang, HAO Xiao-chun, BU Jian-hua, GE Zhong-xue, PAN Qing, WANG Ming

***Chinese Journal of Energetic Materials*, 2014, 22(5): 719–721**

Boron triazide($B(N_3)_3$) was synthesized via low-temperature reaction in acetonitrile with trimethylsilylazide and boron tribromide as starting materials.

One-pot Synthesis of 2,4,5-Trinitroimidazole

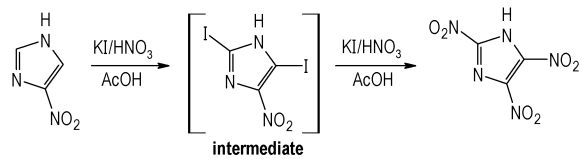

JIN Xing-hui, HU Bing-cheng, LIU Zu-liang, Lü Chun-xu

***Chinese Journal of Energetic Materials*, 2014, 22(5): 722–724**

2,4,5-Trinitroimidazole from 4-nitroimidazole was synthesized by an improved one-pot method.
